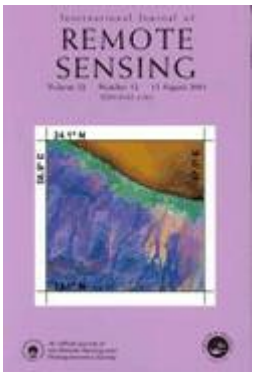

Forward Modeling of Linear Mixing in Thermal IR Temperature Retrieval

Journal:	*International Journal of Remote Sensing*
Manuscript ID:	draft
Manuscript Type:	Special Issue Paper
Date Submitted by the Author:	n/a
Complete List of Authors:	McCabe, Matthew; Los Alamos National Laboratory, International Space and Response (ISR) Balick, Lee; Los Alamos National Laboratory, International Space and Response (ISR) Theiler, James; Los Alamos National Laboratory, International Space and Response (ISR) Gillespie, Alan; University of Washington, Earth and Space Sciences Mushkin, Amit; University of Washington, Earth and Space Sciences
Keywords:	LAND SURFACE TEMP, MODELLING, THERMAL INFRARED
Keywords (user defined):	LAND SURFACE TEMP, MODELLING, THERMAL INFRARED

Forward Modeling of Linear Mixing in Thermal IR Temperature Retrieval

M. F. MCCABE†*, L. K. BALICK†, J. P. THEILER†, A. R. GILLESPIE‡ and A. MUSHKIN‡

† Space and Remote Sensing Sciences Group, Los Alamos National Laboratory, Los Alamos, NM 87545

‡ Department of Earth and Space Sciences, University of Washington, Seattle, WA 98195

Correspondence: * M. F. McCabe.

Email: mmccabe@lanl.gov

Virtually all remotely sensed thermal IR pixels are, to some degree, mixtures of different materials or temperatures: real pixels are rarely thermally homogeneous. As sensors improve and spectral thermal IR remote sensing becomes more quantitative, the concept of homogeneous pixels becomes inadequate. Quantitative thermal IR remote sensors measure radiance. Planck's Law defines a relationship between temperature and radiance that is more complex than linear proportionality and is strongly wavelength dependent. As a result, the area averaged temperature of a pixel is not the same as the temperature derived from the average radiance or radiance spectra, even for blackbodies: this difference is often an error in temperature retrieval from radiance measurements. This paper uses simple linear mixing of pixel elements (subpixels) to examine the impacts of pixel mixtures on temperature retrieval and ground leaving radiance. The results show that for a single material with one temperature distribution and with a subpixel temperature standard deviation of 6K (daytime images), the effects of subpixel temperature variability are small but can exceed 0.5K in the 3-5μm band and about a third of that in the 8-12μm band. For pixels with a 50:50 mixture of materials (two temperature distributions with different means) the impact of subpixel radiance variability

on temperature retrieval can exceed 6K in the 3-5μm band and 2K in the 8-12μm ban. Temperature distributions obtained from high resolution thermal images as well as specified distributions of temperature are used as inputs to the model. The model results are compared to broadband thermal images of plowed soil and senesced barley. In addition, a theoretical framework for quantifying the effect of non-homogeneous temperature distributions for the case of a binary combination of mixed pixels is derived, with results shown to be valid for the range of standard deviations and temperature differences examined herein.

Keywords: Thermal infrared; Linear mixing; Planck function; Mixed pixels; Surface temperature

1 INTRODUCTION

1.1 Background

The retrieval of land surface temperature is an objective for many quantitative earth observing satellite systems. Retrieval on the order of 1K seems achievable, but validation studies are generally and logically performed in areas of nearly uniform surfaces. Complexities arising from mixed pixels are usually neglected although they have long been known to be a problem for quantitative retrievals. Regardless of the spatial scale, variations of real surfaces nearly always exist. Even when the surface materials can be considered uniform, variations of subpixel surface geometry, weathering, shadows and micro-shadows etc. are generally present to some degree. If more than one material is present, even if they have the same emissivity, it is unlikely that they will have the same surface temperature. Subpixel radiance variations in the thermal infrared can arise from having emissivity variations (different materials) in the pixel and from the materials having different temperatures: typically both occur. Thermal emittance observations are impacted by both emissivity and temperature through the Planck's function, $B(T,\lambda)$:

$$M = \varepsilon \int_{\lambda_1}^{\lambda_2} B(T_s, \lambda) d\lambda \quad (1)$$

where M is the emittance of a surface (W/m^2) for a spectral band from wavelength λ_1 to λ_2, ε is the band emissivity, and B (T_s,λ) is the blackbody emittance at the surface temperature, T_s. The classical challenge in quantitative thermal IR remote sensing is in separating T_s and ε (temperature-emissivity separation, TES) , thereby retrieving temperature and emissivity. TES is difficult even for uniform pixels because the separation is mathematically underspecified: a priori knowledge of either temperature or emissivity or an assumption is needed. The problem becomes more complicated with mixed pixels: the combined radiance not only depends on the proportions of surface materials but also on the temperature distributions of each of those materials.

Sources of variations within pixels are complex and they can interact in non-linear ways. They include the presence on multiple material types with different emissivity, but even a single material type may have varying emissivity due to small scale variations of composition and surface conditions. Surface roughness at scales much larger than the measuring wavelengths creates non-linear interactions between surface facets that drive the emissivity toward a blackbody. It also results in directional variations of radiance even if the emissivity is locally non-directional. Surface temperatures are the result of non-linear, three dimensional energy transfers that are themselves time dependent and a function of the surface and subsurface thermal properties of the materials, the atmospheric boundary layer meteorology, and thermal history. Coherent boundary layer turbulence can lead to spatial/temporal fluctuations of temperature that can be important at high resolutions. Research has been initiated to develop a forward model of spectral ground leaving radiance for realistic pixels integrating these effects. The work presented here represents the completion of the first phase of this modeling: linear mixing of radiance from pixel sub-components.

Sources of small scale emissivity and temperature variation have long been known qualitatively. The development of well calibrated high spatial resolution broadband, multi-spectral and hyper-spectral thermal

IR sensors, has lead to increased capabilities and expectations for quantitative thermal IR remote sensing. A number of studies have been published aimed at quantifying these capabilities. There is a long history of studying effects of angular variation in the ground leaving radiance of heterogeneous surfaces, mostly for vegetation canopies, including Fuchs et al. (1967), Kimes et al. (1980), Balick and Hutchison (1986), Smith et al. (1997), Sobrino and Cuenca (1999), Lagouarde et al. (2000), Chebouni et al. (2001), Su et al. (2003), Coret et al. (2004) and Cuenca and Sobrino (2004). Because of this work in vegetation and the fact that the geometry in vegetation-soil complexes is a volume emission problem, vegetated surfaces are not the focus of this particular investigation. More general studies of the angular variation of emissivity and radiance that include the solid ground surface include Snyder and Wan (1998), McAtee et al. (2003) and Chen et al. (2004) among others. Zhang et al. (2004) looked at emissivity scaling issues with mixed solid surface pixels. Small scale time dependence (minutes) of surface temperature was studied quantitatively by Katul et al. (1998), Balick et al. (2002), Jeffery et al. (2002), and Kustas et al. (2002). Problems in validating land surface temperature retrieval algorithms with ground measurements due to temporal and spatial thermal variability have been demonstrated by Sobrino et al. (2006).

1.2 Objectives

The broad objective of this paper is to describe the impact of mixed pixels on broadband temperature retrieval using a linear mixing model. The purpose of calibrated broadband sensors is primarily temperature retrieval: they do not normally provide emissivity information. Results are shown for the mid IR (3-5μm) and longwave IR (8-12μm). The work is mainly aimed at small pixels that might be obtained by airborne sensors, on the order of one to a few square meters, but it is relevant to mixing within larger pixels. Arbitrary materials, proportions, and temperature distributions are used in the model to examine the impact of mixed pixels on temperature retrievals and the sensitivity of temperature retrieval to model inputs. Then we apply the model to

two high resolution images (~ 2mm) as a reality check, if not validation. Finally, we briefly examine the implications of mixed pixels on spectral thermal IR measurements.

2 METHOD

2.1 Linear mixing model

The model assumes that a pixel is comprised of an ensemble of subpixels of one or more material. Each material is defined by an emissivity value and a temperature distribution: the temperature distribution is specified with a mean, standard deviation and a number of subpixels. The impact of mixtures on the difference between average temperature and the temperature retrieved from the average radiance (or ensemble radiant temperature from Norman and Becker, 1995) is examined as a function of temperature distribution properties and material proportions. Here, calculations are done for the 3-5μm and 8-12μm bands and assume an emissivity of 1.0. Pixels are considered to be on the order of meters in dimension, as might be obtained by airborne sensors. Temperature distributions obtained from high resolution thermal images as well as specified distributions of temperature are used as inputs to the model. The specified distributions are assumed to be normally distributed, which while not strictly true in reality, is a close enough approximation so as to be useful for studying model sensitivity. The effects of downwelling radiance and atmospheric transmittance are not considered here but the impact of spatial-temporal fluctuation of skin temperature on skin temperature variability will be discussed.

We recognize that the model is a highly simplified representation of reality. We use it to demonstrate the impact of omnipresent pixel heterogeneity on ground leaving radiance from flat, solid surfaces and subsequently on temperature retrieval. More challenging than creating the model is providing it with sound, realistic inputs and with an understanding of how they vary in reality. Also, variations that occur on a scale of about 1 mm or less are not considered here for several reasons. First, as the scale of the wavelength is

approached, particle scattering effects become important (Vincent and Hunt, 1968; Conel, 1969; and Kirkland et al. 2002). Modeling of this nonlinear process (Mie scattering) has not been comprehensively accomplished for solids. Second, characterizing the constituents for most natural solids at this scale, including its variability, is difficult to impossible, except for a limited number of samples. Third, retrieving temperature or identifying materials at this scale is of limited interest in most remote sensing applications.

The linear mixing model is a model of radiance, not temperature. To convert results to temperature, look-up tables were generated containing the integrated Planck's function radiance as a function of temperature in the 3-5μm and 8-12μm bands (a square wave response function is assumed). High order polynomial equations were then fit to these data to describe temperature as a function of band radiance, and band radiance as a function of temperature.

Table A1. Coefficients for polynomial of form $F = a0 + a1x + a2x^2 + a3x^3 + a4x^4 + a5x^5 + a6x^6$ where F is either determining radiance from temperature (L < T) or temperature from radiance (T < L). b0 terms describe a function of the same form as F but supply the inverse relationship. Coefficients were determined over the defined spectral ranges listed below and are valid in the temperature range 270-330K. The polynomial relationship are also used in Appendix A to approximate first and second derivatives of the Planck function.

L < T	**3-5μm**	**8-12μm**	**T < L**	**3-5μm**	**8-12μm**
a0	131.48301	-122.34352	b0	247.08160	195.17938
a1	-1.8776691	2.2885058	b1	16.903204	1.6173606
a2	0.0086870284	-0.013790340	b2	-2.2102338	-0.011610265
a3	$-6.0438050 \times 10^{-6}$	1.6008487×10^{-5}	b3	0.20261292	6.9150957×10^{-5}
a4	$-5.9776185 \times 10^{-8}$	1.0603946×10^{-7}	b4	-0.011101128	$-2.6325984 \times 10^{-7}$
a5	$1.3562350 \times 10^{-10}$	$-2.5368796 \times 10^{-10}$	b5	0.00032681341	$5.6673097 \times 10^{-10}$
a6	$-3.6142202 \times 10^{-14}$	$1.6898693 \times 10^{-13}$	b6	$-3.9649400 \times 10^{-6}$	$-5.2399755 \times 10^{-13}$

The first set of results to be presented was generated by assigning a normal distribution of temperature (n=1000 subpixels) to a single material and varying the standard deviation. The difference between the mean temperature of the subpixels and the ensemble temperature retrieved from the mean radiance (ΔT) is plotted against the standard deviation. ΔT is the error that results from assuming that the temperature retrieved from the total mixed pixel radiance equals the mean temperature of the subpixels. The second set of results is

produced by sampling normal temperature distributions for each of two materials, then mixing (averaging) the radiance in equal proportion (50:50 mixture), and retrieving temperature. One of the materials is kept at a constant mean temperature (290K) while the other is increased in steps of 5K from 295K to 330K. ΔT is plotted against the difference between the mean temperatures of each material. While both materials have the same standard deviations, different curves are produced for a range of standard deviations. The third set of results is similar to the second except that the materials have a 90:10 proportion with the 10% being warmer than the 90%. Next, the change of ΔT is shown where two materials are mixed in equal proportion but the emissivity of one of the materials is reduced in steps of 0.2. Finally, we show the results of using a temperature distribution taken from real images of a single material at high spatial resolution (< 2mm).

3 RESULTS

3.1 Single material temperature distribution

Recall that ΔT is the difference between the mean temperature of the subpixels and the temperature retrieved from the pixel radiance. To look at the impact of the standard deviation of subpixel temperature, ΔT is plotted against the standard deviation of the temperature distribution for one material in Figure 1a (3-5μm) and Figure 1b (8-12μm). The standard deviation varies between 0K and 12K: a standard deviation of 5K or 6K is probably on the high side for a pixel of uniform material at the meter scale, but it has been observed for materials such as plowed soil and rocky terrain on sunny days. Larger pixels may encounter more variability. For standard deviations likely to be encountered at the meter scale, the impact of varying subpixel temperature on retrievals is minor: less than 0.5K in the mid-IR and less than 0.2K in the longwave IR. When the standard deviation is very large (on the order of 10K), a ΔT of nearly 1.5K in the 3-5μm band and about a third of that in the 8-12μm band is modeled. The apparent outliers in the 3-5μm plot are the result of Gaussian samples

with an unusual number of pixels in the upper tail of the distribution: the 3-5mm band is more sensitive to high values of temperature and it is more likely to occur when the standard deviations are very large. Whether these magnitudes of retrieval errors are important or not depend on the sensor and application, but they can exceed the signal to noise levels of most modern sensors.

3.2 Binary mixtures

Figures 2a (3-5μm) and 2b (8-12μm) show the change of ΔT as the difference of the mean of the temperature distributions of two materials (t), mixed in equal proportions, increasing from 5K to 40K. The standard deviation of the two temperature distributions are kept the same. A mean temperature difference of 40K between materials in a pixel is large at the meter scale but not unreasonable, especially as scales increase. With no temperature variation within materials (standard deviation = 0), ΔT reaches nearly 6K in the 3-5μm band and about a third of that in the 8-12μm band. However, at more modest differences between the means of the temperature distributions the effect is much reduced. When the mean temperatures are 10K apart and the standard deviation is 0K, ΔT is about 0.5K in the 3-5μm band and on the order of 0.1K in the 8-12μm band. Indeed, when the means differ by 10K or less, the effect of having a standard deviation of about 2.5K is larger than the effect of having different mean temperatures. As expected, the effect of increasing the standard deviation is nearly independent of the difference between means.

A 50:50 mixture represents the largest mixture effect for two materials in a pixel. Figure 3a (3-5μm) and Figure 3b (8-12μm) contain plots similar to Figure 2a and Figure 2b except that the mixture is 90:10 with the 10% portion being the warmer or variable temperature component. This is analogous to having a warm, subpixel object in the pixel that composes 10% of the pixel area. ΔT in this case is slightly less than half of the 50:50 mixture when the standard deviation is zero.

In Figures 1-3 it appears that ΔT varies quadratically with the standard deviation and the difference of temperature distribution means. In fact, it can be shown that for binary mixtures, variation in ΔT can be approximated by:

$$\Delta T = c\left(p(1-p)t^2 + p\sigma_1^2 + (1-p)\sigma_2^2\right) \quad (2)$$

where σ_1 and σ_2 are the standard deviations, p the proportion of one of the materials, t is the difference in the mean temperature distributions, and c is a function of the first and second derivatives of the Planck's function at the mean temperature, integrated over the wavelengths of interest. The equation is fully derived in Appendix A. For the cases shown in Figure 2 and Figure 3, the value of c for a representative temperature of 290K (c varies with mean temperature T_o) is approximated as 0.016098 K^{-1} in the 3-5μm band and 0.005444 K^{-1} in the 8-12μm band. It should be noted that Eq. 2 is only formally valid for blackbodies in the small σ and t regime, as can be observed in Figures 2 and 3, but the expression generally provides a good approximation for the temperature ranges used here.

3.3 Emissivity changes

Figure 4 shows the variation of ΔT for two materials in equal proportions and at the same temperature, but the emissivity of the second material is reduced in steps of 0.2. The 3-5μm band shows a temperature decrease of 1.4K when the emissivity of one of the materials is 0.9 and 1.0 for the other. If there were only a single material, the change of temperature (ΔT) between an emissivity of 1.0 and 0.9 would be twice that of the mixture, or -2.7K. The same calculations for the 8-12μm band show that ΔT for the mixture with one of the materials at an emissivity of 0.9 is 2.9K. For a single material, that change in emissivity results in a ΔT of -5.8K. The greater sensitivity of temperature retrieval to emissivity at longer wavelengths shows one of the few advantages in temperature retrieval of the 3-5μm band: temperature retrieval is about half as sensitive to errors in emissivity estimation as for the 8-12μm band (Mushkin et al., 2005).

3.4 High resolution thermal images

Figures 5 and 6 show high resolution thermal images taken with a microbolometer thermal infrared imager near Barrax, Spain. The detector is a 320 x 240 array with precision less than 0.1K. The image was taken at nadir and the area of the images is about 0.4m x 0.6m and pixel separation distance is less than 2mm. The spectral response of the sensor is not known but it is given by the manufacturer as 8-14μm. Figure 5 is an image of plowed soil and has a mean, standard deviation, range, and skewness of 314.6K, 3.6K, 24.2K, and -0.4K^3 respectively. ΔT for this image in the 8-14μm band is 0.05K and is consistent with the model. If we assume that the temperature reported by the camera is the true kinetic temperature, and if the image data were taken in the 3-5μm band, ΔT would be 0.18K. Figure 6 is an image of senesced barley with imaging geometry similar to Figure 5. It is neither a flat surface nor uniform material but the material below the grain heads is largely dry leaves so the emissivity is probably nearly uniform. The mean, standard deviation, range, and skewness of this image is 306.9K, 2.5K, 16.0K and 0.8K^3 respectively. ΔT for this image in the 8-14μm band is 0.03K, essentially in the noise but consistent with the model. If it were obtained in the 3-5μm band, ΔT is calculated to be 0.08K.

4 DISCUSSION AND CONCLUSION

The work presented her focuses on estimating ΔT – the difference between the mean temperature and the temperature retrieved from the radiance of mixed pixel. The simplest form of subpixel variation is when there is one material with varying temperature. In this case, ΔT is quite small under modest levels of subpixel variation at meter scales: a few tenths of a degree. However, it can become more significant (on the order of 1K) for cases where the variability is quite large. For binary mixed pixels, two materials with different temperature distribution means, ΔT is still rather small for most conditions, at least for the longer wavelengths: ΔT stays below 1K until the mean temperature difference reaches roughly 25K. ΔT can become

large when subpixels of materials with considerably different mean temperatures are present. At a difference of 40K, ΔT is about 6K in the 3-5μm band and 2K in the 8-12μm band. Roughly, model calculations of ΔT are three times larger in the 3-5μm band than the 8-12μm band when subpixel variability is the same.

These results lead to a conclusion that the effect of subpixel mixing is small for small pixels under a wide range of realistic circumstances. However, errors of temperature retrievals can become large under conditions of large but realistic subpixel temperature variation such as when subpixel heat sources are present in the pixel, especially in the 3-5μm band. Field observations indicate that temporal fluctuations at a point during the day often fluctuate by several degrees: in-situ field measurements have observed fluctuations of 9 or 10K on several surfaces. If these occur at pixel or subpixel scales, these fluctuations would add significantly to the variability of temperature in the pixel. Indeed, the temperature variability encountered by real sensors would depend strongly on spatial scales. It can be expected that temperature variation in large pixels is usually greater than variability of small pixels, but the spatial scaling of temperature or emissivity is a complex problem. Temperatures are commonly retrieved from satellite sensors at 1km resolution. What temperature or material variations exist within that $1km^2$ area? What scales of variation are important? Can a 90m x 90m pixel effectively define subpixel temperature variation? Is 10m GSD adequate, 1m, or even 1 mm? To an extent the answer lies in what is in a particular pixel but the issue is a general one.

Exercising a simple model is a simple task: much more difficult is in knowing what realistic inputs to the model are. Linear mixing applies to flat surfaces, but realistic surfaces are rarely flat. In the two examples given in Figures 4 and 5 the surfaces are far from flat: the soil heights vary by 10 cm (roughly) and the barley canopy is really a volume emitter 40cm to 50cm deep. Eventually, this model will be integrated with a model of the effects of solid surface roughness, at which point the mode then becomes non-linear. The early stages of this model are described by Danilina et al. 2006. Ultimately, a model of turbulence induced spatial/temporal skin temperature fluctuations will be added (Balick et. al,. 2006).

Finally, a comment about temperature retrieval from mixed pixels using hyperspectral thermal data is appropriate. A common approach uses what is sometimes called "Planck's function draping" in which the best fit of the Planck's function to the radiance spectra continuum (excluding spectral features) determines the temperature. This technique has a problem for mixed pixels because the sum of two Planck's functions is not a Planck's function. For a blackbody pixel that has an average temperature of 300K but has a mixture with half at 285K and half at 315K, ΔT is about 2K in the mid-IR and nearly 1K in the longwave IR. If the mixture is at temperatures of 280K and 320K, ΔT increases to about 6K in the 3.5μm band and 2K in the 8-12μm band. These numbers are similar to the broadband results presented in this paper: any advantage to using spectral data would come from improved knowledge of emissivity.

ACKNOWLEDGMENT

The authors thank the Global Change Unit at the University of Valencia, Dr. Sobrino, staff and students, for the opportunity to participate in the SEN2FLEX field campaign organized by the European Space Agency. They graciously shared a microbolometer thermal IR camera which provided much useful information on temperatures at high spatial and temporal resolution. We thoroughly enjoyed their support and collaboration. This work was funded by the U. S. Department of Energy, Office of Nonproliferation Technology Development, under contract W-7405-ENG-36 with the University of California and contract DE-AC52-06NA25396 with Los Alamos National Security, LLC.

REFERENCES

Balick, L. K. and Hutchison, B. A., 1986, Directional thermal infrared exitance distributions from a leafless deciduous forest. *IEEE Transactions on Geosicence and Remote Sensing,* **24**:5, 693-698.

Balick, L. K. Jeffery, C. A., and Henderson, B. G., 2003. Turbulence induced spatial variation of surface temperature in high resolution thermal IR satellite imagery. *Remote Sensing for Agriculture, Ecosystems, and Hydrology IV*, Edited by Owe, M., D'Urso, G. and Toulios, L., Proceedings of SPIE Vol. 4879, 221-230.

Balick, L. K., Jeffery, C. A., and McCabe, M. F., 2006. Understanding Thermal Variability Using a new Dynamical Model of the Surface Skin Temperature and Turbulent Near Atmosphere. American Geophysical Union Fall 2006 Fall Meeting, Dec, 2006.

Chebouni, A., Nouvellon, Y., Kerr, Y. H., Moran, M. S., Watts, C. J., Prevot, L., Goodrich, D. C. and Rambal S., 2001, Directional effects on radiative surface temperature measurements over a semi-arid grassland site. *Remote Sensing of Environment*, **76**:3, 360-372.

Chen, L. F., Li, Z. L., Liu, Q. H., Chen, S., Tang, Y., and Zhong, B., 2004. Definition of component effective emissivity for heterogeneous and non-isothermal surfaces and its approximate calculation. *International Journal of Remote Sensing*, **25**:1, 231-244.

Conel, J. E., 1969, Infrared emissivities of silicates: experimental results and a cloudy atmosphere model of spectral emission from condensed particle mediums, *Journal of Geophysical Research*, **74**:6, 1614-1634.

Coret, L., Briottet, X., Kerr, Y. H.,and Chibouni, A., 2004, Simulation study of view angle effects on thermal infrared measurements over heterogeneous surfaces. *IEEE Transactions on Geosicence and Remote Sensing,* **42**:3, 664 - 671.

Cuenca, J. and Sobrino, J. A., 2004, Experimental measurements for studying angular and spectral variation of thermal infrared emissivity. *Applied Optics*, **43**, 4598-460.

Danilina, I., Mushkin, A., Gillespie, A. R., O'Neal, M., Abbott, E. A., and Balick, L. 2006, Roughness effects on sub-pixel radiative temperature dispersion in a kinetically isothermal surface, *Proceedings of Recent Advances in Quantitative Remote Sensing II*, 25-29 September, 2006, Valencia, Spain.

Fuchs, M., Kanemasu, E. T., Kerr, J. P., Tanner, C. B., 1967, Effect of viewing angle on canopy temperature measurements with infrared thermometers. *Agronomy Journal*, **59**, 494-496.

Jeffery, C. A., Balick, L. K. and Henderson, B. G., 2002, Modeling turbulence induced skin temperature fluctuations of a bluff-rough surface using surface renewal theory. *American Geophysical Union*, Fall Meeting, San Francisco, CA, Dec. 6-10, 2002.

Katul, G. G., Schieldge, J., Hseih, C., and Vidakovic, B., 1998, Skin temperature perturbations induced by surface layer turbulence above a grass surface. *Water Resources Research*, **34**:5, 1265-1274.

Kimes, D. S. Idso, s. B., Pinter, P. J,. Reginato, R. J., and Jackson, R. D., 1980, View angle effects in the radiometric measurement of plant canopy structure. *Remote Sensing of Environment*, **10**, 273-284.

Kirkland L., Herr, K., Keim, E., Adams, P., Salisbury, J., Hackwell, J., and Treiman, A. 2002, First use of an airborne thermal hyperspectral scanner for compositional mapping. *Remote Sensing of Environment*, **80**:3, 447-459.

Kustas, W. P., and Norman, J. M., 2000, Evaluating the effects of subpixel heterogeneity on pixel average fluxes. *Remote Sensing of Environment*, **7 4**, 347-342.

Kustas, W. P., Prueger, J. H. and Hipps, L. E., 2002, Impact of using time averaged inputs for estimating sensible heat flux of riparian vegetation using radiometric surface temperature. *Journal of Applied. Meteorology*, **41**, 319-331.

Lagouarde, J. P., Mallans, H., Moreau, P.,Guyon, D., and Coraboeuf, D., 2000,. Experimental study of brightness temperature angular variations of Maritime Pine (Pinus pinaster) stands. *Remote Sensing of Environment*, **72**:1, 17-34.

McAtee, B. K., Prata, A. J., and Lynch, M. J., 2003, The angular behavior of emitted thermal infrared radiation (8-12μm) at a semiarid site. *Journal of Applied. Meteorology*, **42**, 1060 – 1071.

Mushkin, A., Balick, L. K. and Gillespie, A. R., 2005, Extending surface temperature eand emissivity retrieval to the mid-infrared (3-5μm) using the Multispectral Thermal Imager (MTI). *Remote Sensing of Environment*, **98**, 141-151.

Norman, J. M., and Becker, F., 1995, Terminology in the thermal infrared remote sensing of natural surfaces, *Agricultural and Forest Meteorology*, **77,** 153-166.

Smith, J. A., Chauhan, N. S., Schmugge, T. J. and Ballard, J. R., 1997, Remote sensing of land surface temperature: the directional viewing effect. *IEEE Transactions of Geoscience and Remote Sensing*, **35**:4, 972-974.

Sobrino, J. A., and Cuenca, J. 1999, Angular variation of the thermal infrared emissivity for some natural surfaces from experimental measurements. *Applied Optics*, **38**:18, 3931-3936.

Sobrino, J. A., Jimenez-Munoz, J. C., TZarco-Tejeda, P. J., Sepulcre-Canto, G., and de Miguel, E., 2006, Land surface temperature derived from airborne hyperspectral scanner thermal infrared data, *Remote Sensing of Environment*, **102**, 99-115.

Su, L. Li, X, Liang, S., and Strahler, A. H., 2003, Simulation of scaling effects on thermal emission from non-isothermal pixels with the typical three-dimensional structure. *International Journal of Remote Sensing,* **24**:19, 3743-3753.

Snyder, W, C. and Wan, Z., 1998, BRDF models to predict spectral reflectance and emissivity in the thermal infrared. *IEEE Trans on Geosicence and Remote Sensing.* **36**:1, 214-225.

Vincent, R. K., and Hunt, G., R., 1968, Infrared reflectance from mat surfaces. *Applied Optics*, **7**:1, 53-59.

Zhang, R. H., Li, Z. L., Tang, X. Z., Sun, H. B., Zhu, C., and Zhu, Z. L., 2004,. Study of emissivity scaling and relativity of homogeneity of surface temperature, *International Journal of Remote Sensing*, 25:1, 245-259.

APPENDIX A

If B(T) is the total pixel radiance over the band of interest due to a pixel at temperature T, and if h(T) is the distribution of temperatures in the pixel of interest, then we can write;

$$1 = \int h(T)dT$$
$$T_o = \int T.h(T)dT \qquad \text{A1}$$

Where T_o is the mean temperature in the pixel, and

$$R_{pix} = \int B(T)h(T)dT \qquad \text{A2}$$

is the pixel radiance. Further, we can write:

$$T_B = B^{-1}\left[\int B(T)h(T)dT\right] \qquad \text{A3}$$

where B^{-1} is the inverse of the Planck function and T_B is the brightness temperature of the pixel i.e. it is the temperature that will be retrieved from a measurement of radiance over a given waveband. Then $\Delta T = T_B - T_o$ is the error we make in estimating the mean temperature T_o from the radiance R_{pix}. To estimate the magnitude of this error, we begin with a Taylor series expansion on A2 about $z = T\text{-}T_o$. Considering only the leading 2 orders leads, we obtain:

$$R_{pix} = B(T_o)\int h(T)dT + B'T_o\int zh(T)dT + Th(T)dT + \frac{1}{2}B''T_o\int z^2h(T)dT + ... \qquad \text{A4}$$

Using the properties of h(T) defined in A1, this simplifies to:

$$R_{pix} = B(T_o) + \frac{1}{2}B''(T_o)\int (T-T_o)^2 h(T)dT = B(T_o) + \frac{1}{2}B''(T_o)\sigma_{eff}^2 \qquad \text{A5}$$

where $\sigma_{eff}^2 = \left\langle (T-T_o)^2 \right\rangle$ describes the temperature variance in the pixel. Now, writing $R_o = B(T_o)$ as the radiance that would be observed in a pixel of uniform temperature T_o, then:

$$\Delta T = T_B - T_o \approx \frac{B(T_B) - B(T_o)}{B'(T_o)} = \frac{R_{pix} - R_o}{B'(T_o)} \quad \text{A6}$$

Substituting values for R_{pix} and R_o defined above yields:

$$\Delta T = \frac{R_{pix} - R_o}{B'(T_o)} = \frac{B(T_o) + \frac{1}{2}B''(T_o)\sigma_{eff}^2 - B(T_o)}{B'(T_o)} = \frac{\frac{1}{2}B''(T_o)\sigma_{eff}^2}{B'(T_o)} \quad \text{A7}$$

In terms of defining the temperature variance within a pixel, if we are given two temperatures, T_1 and T_2, the variance about the mean temperature T_o can be expressed:

$$\left\langle (T - T_o)^2 \right\rangle = p(T_1 - T_o)^2 + (1-p)(T_2 - T_o)^2 \quad \text{A8}$$

where T_1 and T_2 are the temperatures of each area and $T_o = pT_1 + (1-p)T_2$ is the average temperature, straightforward algebraic manipulation leads to:

$$\left\langle (T - T_o)^2 \right\rangle = p(1-p)t^2 \quad \text{A9}$$

where $t = T_2 - T_1$. In the more general case that there is variation in each of the areal components, such that these areas have mean temperatures T_1 and T_2, and variances σ_1 and σ_2, it can be shown that:

$$\left\langle (T - T_o)^2 \right\rangle = p(1-p)t^2 + p\sigma_1^2 + (1-p)\sigma_2^2 \quad \text{A10}$$

which gives an estimate of $\left\langle (T - T_o)^2 \right\rangle$, or the effective standard deviation of a binary mixture, in terms of pixel proportion and difference in mean temperature. Therefore, taking our result from A7 for the first and second differentials of the Planck function, and combining with knowledge of the variance of the temperature distributions (σ_{eff}^2), we can define the general expression for the difference in temperature ΔT as:

$$\Delta T = c{\sigma_{eff}}^2 = c\left\langle (T - T_o)^2 \right\rangle = \frac{\frac{1}{2}B''(T_o)}{B'(T_o)}\left(p(1-p)t^2 + p\sigma_1^2 + (1-p)\sigma_2^2\right) \quad \text{A11}$$

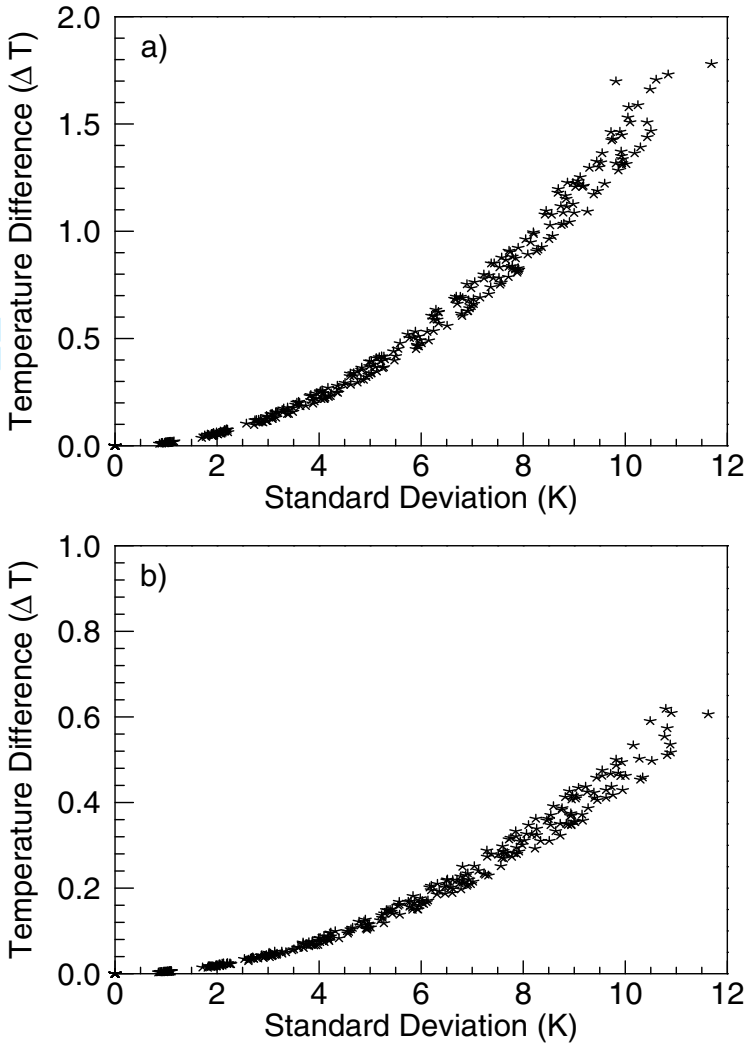

Figure 1. ΔT for one material as a function of its standard deviation of subpixel temperature in the a) 3-5μm band and b) 8-12μm.

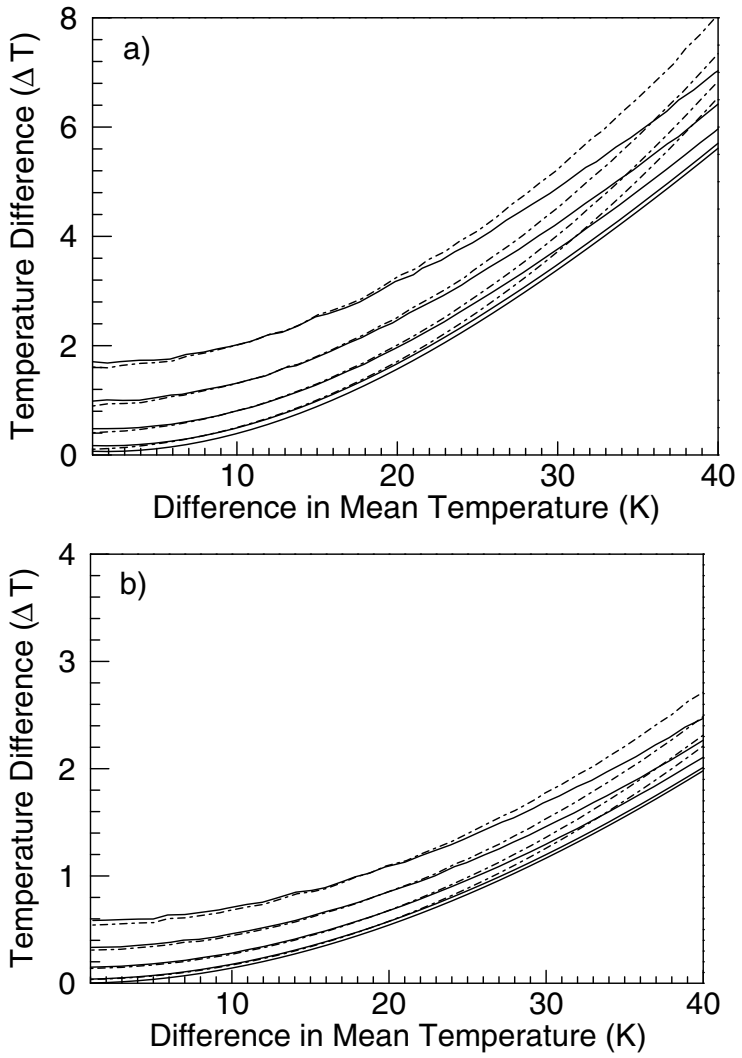

Figure 2. ΔT as a function of the difference between mean temperatures in a 50:50 mixture for different standard deviations in the a) 3-5μm band and b) 8-12μm. The upward progression of curves represent increasing standard deviations of 0, 2.5, 5 and 10 (solid lines). Approximations for ΔT as a function of the difference in the temperature means and material proportions as derived in Appendix A are also included for comparison, for standard deviations greater than 0 (dashed lines).

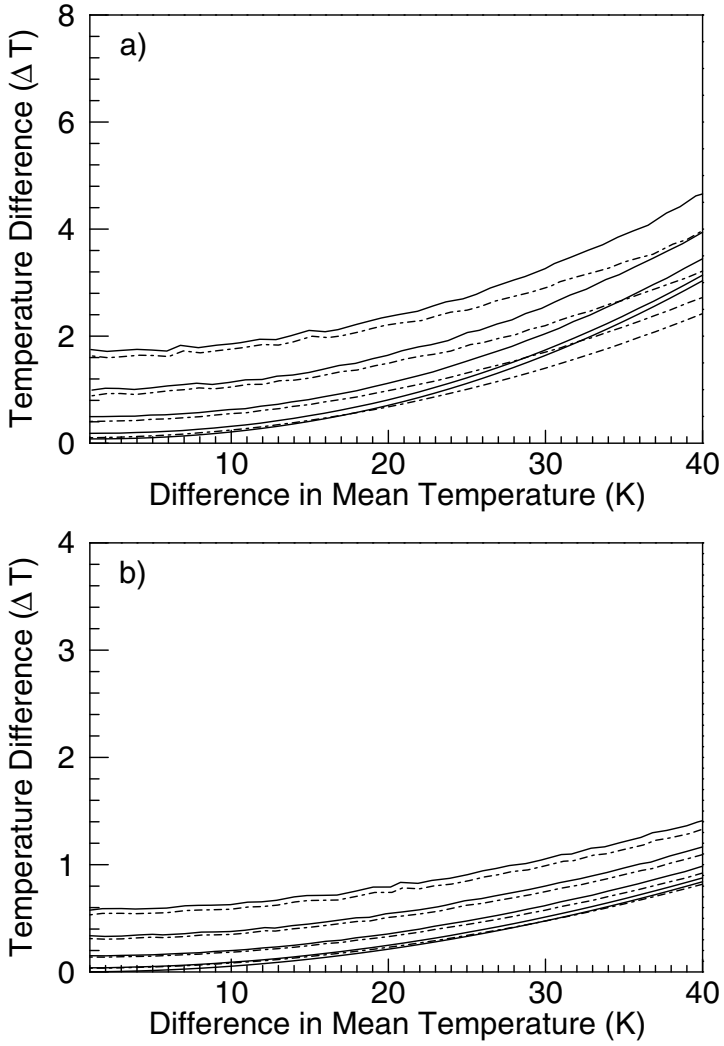

Figure 3. ΔT as a function of the difference between mean temperatures in a 90:10 (warm) mixture and for different standard deviations in the a) 3-5μm band and b) 8-12μm. The upward progression of curves represent increasing standard deviations of 0, 2.5, 5 and 10 (solid lines). Approximations for ΔT as a function of the difference in the temperature means and material proportions as derived in Appendix A are also included for comparison, for standard deviations greater than 0 (dashed lines).

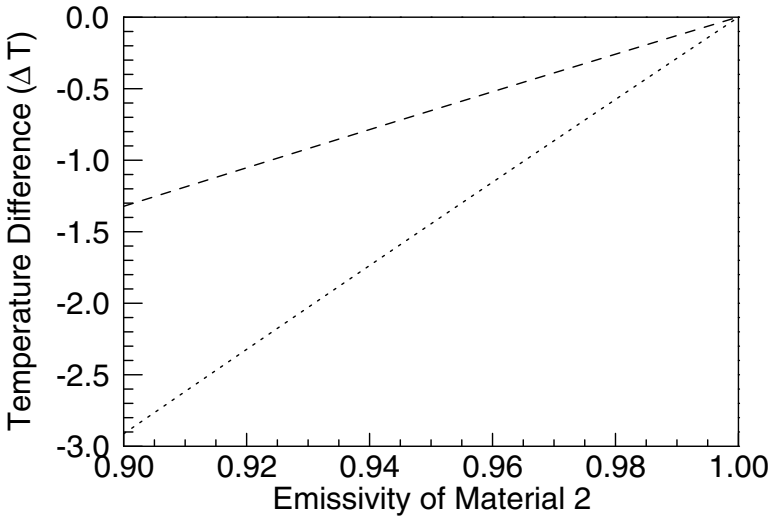

Figure 4. ΔT of a 50:50 mixture of two materials with the same temperature distributions, except the emissivity of one of the materials is varied for the 3-5μm (dotted) and 8-12μm (dashed) spectral range.

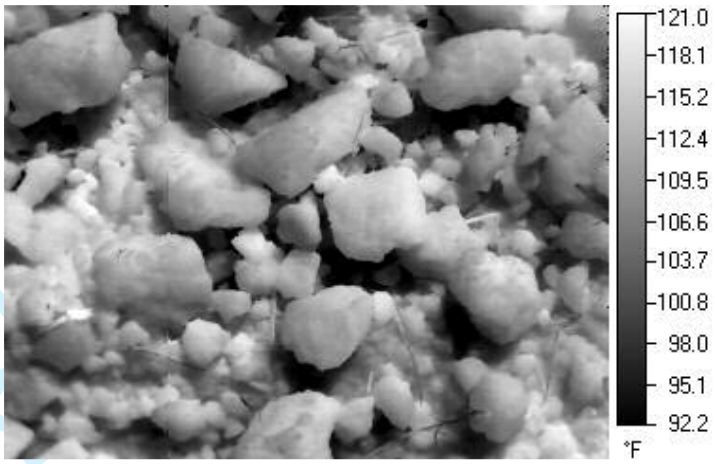

Figure 5. High resolution (< 2mm) thermal IR image of plowed soil (nominally 8-14μm).

Figure 6. High resolution (< 2mm) thermal IR image of senesced barley (nominally 8-14μm).